Asian Journal of Chemistry; Vol. 38, No. 9 (2026), 2485-2491
ASIAN JOURNAL OF CHEMISTRY
https://doi.org/10.14233/ajchem.2026.36430

Exploration of Novel Thiazole Scaffolds with Potential Therapeutic Applications

CHANDRAVADIVELU GOPI[1,*], MAGHARLA DASARATHA DHANARAJU[2], EETHAKOTA PARIMALA NAGA DEVI[1], IRPA SUPRIYA[1] and GULLAPUDI DURGA PRAVALLIKA[1]

[1]Department of Pharmaceutical Chemistry, School of Pharmacy, Godavari Global University, Rajamahendravaram-533296, India
[2]Research Lab, School of Pharmacy, Godavari Global University, Rajamahendravaram-533296, India

*Corresponding author: E-mail: gopic@ggu.edu.in

Received: 14 May 2026 *Accepted*: 20 August 2026 *Published online*: 5 September 2026 AJC-22477

This study focuses on the synthesis and evaluation of the antimicrobial, anti-inflammatory and antipyretic activities of novel thiazole-based Schiff base derivatives (**S1-S6**). The compounds were synthesized through condensation reactions between 2-aminothiazole and several aromatic aldehydes. Structural characterization of the synthesized derivatives was carried out using FTIR, ^{13}C NMR, ^{1}H NMR, mass spectrometry techniques and elemental analysis. Initially, thiazole-based Schiff base derivatives therapeutic activities were assessed from AutoDock score after the successful binding with *Staphylococcus aureus* DNA gyrase B and cyclooxygenase 2. The synthesized derivatives were also evaluated for antimicrobial, anti-inflammatory and antipyretic activities using *in vitro* and *in vivo* methods. Compounds **S6** and **S1** showed the highest activity, possibly due to the thiazole nucleus linked to furan and substituted aromatic rings. The experimental findings were consistent with the *in silico* molecular docking results.

Keywords: Thiazole, Schiff base derivatives, Antimicrobial activity, Anti-inflammatory activity, Anti-pyretic activity.

INTRODUCTION

Thiazole is a five-membered aromatic heterocycle containing one sulphur and one nitrogen atom within its ring system [1]. The thiazole nucleus occurs in several biologically active natural products, vitamins and therapeutic agents [2]. Its presence in clinically important drugs has established thiazole as an important pharmacophore in medicinal chemistry [3]. Thiazole derivatives exhibit a broad range of biological activities, including antimicrobial [4], anti-inflammatory [5], antipyretic [6], antitubercular [7], antiviral [8] and anticancer activities [9]. These properties have encouraged the development of structurally diverse thiazole derivatives for potential therapeutic applications.

Schiff bases are an important class of compounds in organic and medicinal chemistry, generally synthesized through the condensation of primary amines with aldehydes or ketones [10,11]. The simplicity and versatility of this reaction allow the incorporation of diverse aromatic, heterocyclic and aliphatic substituents [12]. Their structural flexibility and tunable electronic properties have led to their wide application in organic synthesis, coordination chemistry and medicinal chemistry [13-15]. Schiff base derivatives have demonstrated antibacterial [16], antifungal [17], antiviral [18], anticancer [19], anti-inflammatory [20], antioxidant [21], antimalarial [22] and enzyme-inhibitory activities [23].

Thiazole–Schiff base hybrids provide an opportunity to combine the biological properties of the thiazole nucleus with the structural and electronic characteristics of the azomethine group. Recent studies [24] have reported thiazole containing compounds with anti-inflammatory activity associated with cyclooxygenase (COX) and lipoxygenase (LOX) pathways. Structural modification of the thiazole nucleus can influence the biological activity and molecular interactions of these compounds. Despite extensive studies on thiazole derivatives and Schiff bases, the biological activity of thiazole-based Schiff base derivatives varies with the nature and position of substituents. Systematic synthesis and biological evaluation can provide useful information on their structure–activity relationships. Molecular docking studies can further provide insight into their possible interactions with selected biological targets.

In the present study, novel thiazole-based Schiff base derivatives (**S1-S6**) were synthesized and evaluated for anti-

microbial, anti-inflammatory and antipyretic activities using *in vitro* and *in vivo* methods. Molecular docking studies were performed to examine their possible interactions with the selected biological target. The study aims to identify promising thiazole–Schiff base derivatives with potential antimicrobial, anti-inflammatory and antipyretic activity.

EXPERIMENTAL

The chemicals used in this study were obtained from Sigma-Aldrich, Ranbaxy and Dr. Reddy's Laboratories and were of laboratory grade. The synthesized Schiff base derivatives were characterized by FT-IR (Perkin-Elmer in the range 4000-400 cm^{-1}), ^1H NMR (Bruker, 400 MHz, $CDCl_3$), mass spectrometry (Shimadzu) and CHN analysis (Perkin-Elmer 2400).

Molecular docking: Molecular docking studies were performed using AutoDock to predict the binding interactions of the synthesized ligands with the target proteins, *S. aureus* DNA gyrase B and cyclooxygenase-2 (COX-2). The crystal structures of the target proteins were retrieved from the Protein Data Bank (PDB), including *S. aureus* DNA gyrase B (PDB ID: 4URO) and cyclooxygenase-2 (PDB ID: 1CX2)**.** Prior to docking, the protein structures were prepared by removing water molecules and other non-essential heteroatoms, followed by the addition of polar hydrogen atoms and Kollman charges. The 2D structures of the five synthesized ligands were drawn using ChemDraw and converted into 3D conformations. The geometrically optimized and energetically most stable conformers were used as input for docking. Docking simulations were performed using the Lamarckian Genetic Algorithm implemented in AutoDock. The ligand-binding sites were defined based on the positions of the respective co-crystallized ligands. For DNA gyrase B (PDB ID: 4URO), the ATP-binding pocket comprising residues Asp81, Arg84, Gly85, Ile86, Lys103, Ser128 and Thr173 was selected for docking. Similarly, for COX-2 (PDB ID: 1CX2), the active-site cavity containing Arg120, Tyr355, Tyr385, Ser530, Val349, Leu352, Trp387, Phe518, Gly526 and Ala527 was used. Grid box center coordinates and dimensions were manually defined to fully encompass the active-site residues before molecular docking. The binding affinity of each ligand was evaluated based on the predicted binding energy (docking score), where more negative binding energy values indicate stronger ligand–protein interactions. The docking results were further analyzed by examining hydrogen bonding, hydrophobic interactions and key amino acid residues involved in ligand binding to compare the binding potential of the synthesized compounds with the target proteins [25].

Synthesis of thiazole–Schiff base derivatives (S1-S6): An equimolar mixture of thiazole-2-amine (0.01 mol) and aromatic aldehyde (0.01 mol) were added gradually to 10 mL of glacial acetic acid contained two-necked round bottom flask. It was refluxed at 80 ºC for 6 h with constant stirring. The resulting solution was left for 10 min. The precipitated solid was filtered, washed with 50 mL of water and recrystallized from ethanol (**Scheme-I**) [26,27].

(Z)-*N*-(Furan-2-ylmethylene)thiazol-2-amine (S1): Off white; yield: 78%; m.p.: 193-195 ºC; FTIR (KBr, ν_{max}, cm^{-1}): 3135 (*str.*, ArC-H), 1507 (*str.*, ArC), 1618 (imine CH=N), 1571 (C=N), 735 (C-S); ^1H NMR (400 MHz, $CDCl_3$, δ ppm): 6.52 (t, 1H, *J* = 9.2 Hz, Ar-H), 6.91 (t, 1H, *J* = 10.5 Hz, Ar-H), 7.64-7.75 (m, 1H, Ar-H), 7.78 (d, 1H, *J* = 7.8 Hz, Ar-H), 7.92 (t, 1H, *J* = 10.2 Hz, Ar-H), 8.62 (s, 1H, imine-H); ^{13}C NMR (400 MHz, DMSO-*d*, δ ppm): 112.72 (C-1), 117.61 (C-2), 118.90 (C-3), 140.32 (C-4), 144.37 (C-5), 146.09 (C-6), 150.18 (C-7), 171.23 (C-8); MS (*m/z*, %): 176 (40) [M^+], 133 (52), 80 (100), 70 (42), 54 (24), 26 (35), 18 (22); Elemental anal. calcd. (found) % for $C_8H_6N_2OS$, (*m.w.* 176): C, 53.92 (53.12); H, 3.39 (3.54); N, 15.72 (15.29); O, 8.98 (8.24); S, 17.99 (17.23).

(Z)-*N*-(4-(Dimethylamino)benzylidene)thiazol-2-amine (S2): Off white; yield: 82%; m.p.: 215-217 ºC; FTIR (KBr, ν_{max}, cm^{-1}): 3142 (*str.*, ArC-H), 1507 (*str.*, ArC), 1613 (imine CH=N), 1542 (C=N), 746 (C-S); ^1H NMR (400 MHz, $CDCl_3$, δ ppm): 3.51 (s, 6H, Ar-H), 6.87 (t, 2H, *J* = 10.8 Hz, Ar-H), 7.56-7.72 (m, 2H, Ar-H), 7.80-7.88 (m, 1H, Ar-H), 7.92-7.99 (m, 1H, Ar-H), 8.32 (s, 1H, imine-H); ^{13}C NMR (400 MHz, DMSO-d_6, δ ppm): 40.20 (C-1,2), 111.61 (C-3,4), 117.45 (C-5), 125.67 (C-6), 128.32 (C-7,8), 140.61 (C-9), 153.26 (C-10),

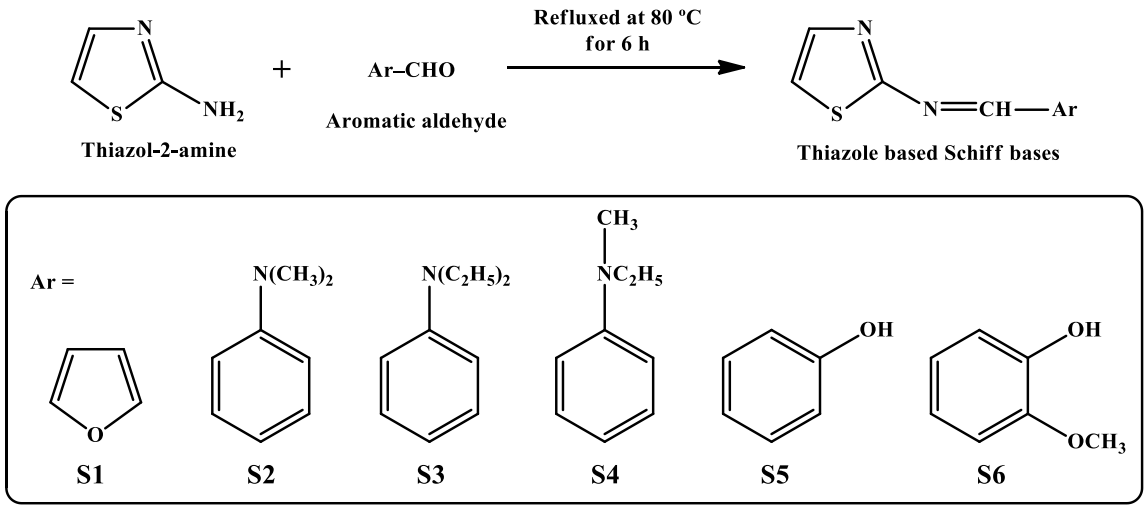

Scheme-I: Synthesis of potent thiazole-based Schiff base derivatives (**S1-S6**)

160.83 (C-11), 172.12 (C-12); MS (*m/z*, %): 231 (40) [M^+], 151 (45), 79 (100), 70 (32), 53 (18), 54 (40), 38 (26); Elemental anal. calcd. (found) % for $C_{12}H_{13}N_3S$, (*m.w*. 231): C, 62.31 (61.97); H, 5.56 (5.39); N, 18.17 (18.34); S, 13.96 (13.42).

(*Z*)-N-(4-(Diethylamino)benzylidene)thiazol-2-amine (S3): Cream; yield: 86%; m.p.: 226-228 ºC; FTIR (KBr, ν_{max}, cm^{-1}): 3127 (*str*., ArC-H), 1552 (*str*., ArC), 1641 (imine CH=N), 1521 (C=N), 729 (C-S); ^{1}H NMR (400 MHz, $CDCl_3$, δ ppm): 1.23-1.32 (m, 6H, *J* = 7.2 Hz, Ali-H), 2.84-3.91 (m, 4H, Ali-H), 6.91 (t, 2H, *J* = 7.5 Hz, Ar-H), 7.52-7.63 (m, 3H, Ar-H), 7.85-7.89 (t, 1H, *J* = 12.5, Ar-H), 8.45 (s, 1H, imine-H); ^{13}C NMR (400 MHz, DMSO-d_6, δ ppm): 12.61 (C-1,2), 47.25 (C-3,4), 111.82 (C-5,6), 117.37 (C-7), 125.17 (C-8), 128.43 (C-9,10), 140.17 (C-11), 148.72 (C-12), 160.61 (C-13), 171.62 (C-14); MS (*m/z*, %): 259 (54) [M^+], 161 (23), 97 (100), 87 (23), 72 (48), 51 (25), 44 (27), 38 (52), 27 (18); Elemental anal. calcd. (found) % for $C_{14}H_{17}N_3S$, (*m.w*. 259): C, 64.83 (64.14); H, 6.61 (6.52); N, 16.20 (16.18); S, 12.36 (12.02).

(Z)-*N*-(4-(Ethyl(methyl)amino)benzylidene)thiazol-2-amine (S4): Pale yellow, yield: 81%; m.p.: 251-253 ºC; FTIR (KBr, ν_{max}, cm^{-1}): 3063 (*str*., ArC-H), 1583 (*str*., ArC), 1603 (imine CH=N), 1538 (C=N), 707 (C-S); ^{1}H NMR (400 MHz, DMSO-d_6, δ ppm): 1.16 (t, 3H, *J* = 7.8 Hz, aliph-H), 2.78 (s, 3H, aliph.-H), 3.53 (t, 2H, *J* = 10.4 Hz, aliph.-H), 6.87 (t, 2H, *J* = 7.2 Hz, Ar-H), 7.59-7.63 (m, 3H, Ar-H), 7.84-7.95 (m, 1H, Ar-H), 8.45 (s, 1H, imine-H); ^{13}C NMR (400 MHz, DMSO-d_6, δ ppm): 12.61 (C-1), 38.26 (C-2), 49.27 (C-3), 111.26 (C-4,5), 117.47 (C-6), 125.93 (C-7), 128.71 (C-8,9), 140.17 (C-10), 151.38 (C-11), 160.50 (C-12), 171.84 (C-13); MS (*m/z*, %): 245 (32) [M^+], 147 (45), 97 (100), 89 (36), 70 (18), 58 (43), 27 (32); Elemental anal. calcd. (found) % for $C_{13}H_{15}N_3S$, (*m.w*. 245): C, 63.64 (63.28); H, 6.61 (6.36); N, 17.13 (17.05); S, 13.07 (12.89).

(*Z*)-2-(Thiazol-2-ylimino)methyl)phenol (S5): Cream, yield: 92%; m.p.: 307-309 ºC; FTIR (KBr, ν_{max}, cm^{-1}): 3052 (*str*., ArC-H), 1531 (*str*., ArC), 1635 (imine CH=N), 1545 (C=N), 737 (C-S), 3517, 1512 (phenolic OH); ^{1}H NMR (400 MHz, $CDCl_3$, δ ppm): 5.85 (s, 1H, phenolic OH-H),7.10-7.13 (m, 2H, Ar-H), 7.58-7.60 (m, 3H, Ar-H), 7.86 (t, 1H, *J* = 7.8 Hz, Ar-H), 8.39 (s, 1H, imine-H); ^{13}C NMR (400 MHz, DMSO-d_6, δ ppm): 117.25 (C-1,2), 120.84 (C-3), 121.13 (C-4), 132.61 (C-5,6), 140.25 (C-7), 160.13 (C-8), 161.53 (C-9), 171.25 (C-10); MS (*m/z*, %): 204 (47) [M^+], 106 (100), 96 (35), 70 (57), 52 (22), 30 (37), 26 (18); Elemental anal. calcd. (found) % for $C_{10}H_8N_2OS$, (m.w. 204): C, 58.80 (58.12); H, 3.95 (3.04); N, 13.73 (13.84); O, 7.83 (7.05); S, 15.70 (15.72).

(Z)-2-Methoxy-4-(thiazol-2-ylimino)methyl)phenol (S6): Yield: 89%; m.p.: 314-316 ºC; Shade: off white; FTIR (KBr, ν_{max}, cm^{-1}): 3038 (*str*., ArC-H), 1573 (*str*., ArC), 1605 (imine CH=N), 1542 (C=N), 712 (C-S), 3525, 1512 (phenolic OH), 2835 (OCH_3); ^{1}H NMR (400 MHz, $CDCl_3$, δ ppm): 3.89 (s, 3H, OCH_3-H), 5.45 (s, 1H, OH-H), 6.93-6.98 (m, 1H, Ar-H), 7.35-7.41 (m, 1H, Ar-H), 7.52-7.57 (m, 1H, Ar-H), 7.61-7.68 (m, 1H, Ar-H), 7.86-7.91 (m, 1H, Ar-H), 8.43 (s, 1H, imine-H); ^{13}C NMR (400 MHz, DMSO-*d*, δ ppm): 56.83 (C-1), 112.53 (C-2), 117.06 (C-3,4), 127.76 (C-5), 130.04 (C-6), 140.28 (C-7), 149.83 (C-8), 151.56 (C-9), 160.25 (C-10), 171.23 (C-11); MS (*m/z*, %): 234 (42) [M^+], 136 (100), 97 (42), 85 (24), 70 (23), 51 (18), 27 (25); Elemental anal. calcd. (found) % for $C_{11}H_{10}N_2O_2S$, (m.w. 234): C, 56.39 (56.08); H, 4.30 (4.16); N, 11.96 (12.41); O, 13.66 (13.25); S, 13.69 (13.45).

Experimental animals: Virgin adult female Wistar albino rats weighing 160-200 g were procured and maintained under standard laboratory conditions at 22 ± 3ºC and 55 ± 5% relative humidity with a 12 h light/dark cycle. The animals were provided standard rat pellet diet and water ad libitum. The experimental protocol was approved by the Institutional Animal Ethics Committee of GIET School of Pharmacy, Rajahmundry, India (GSP/IAEC/2025/02/04). At the end of the study, the animals were euthanized under diethyl ether anesthesia and the ovaries were carefully excised for further analysis [28].

Biological activities

Antimicrobial activity

Zone of inhibition: The antimicrobial activity of the synthesized thiazole–Schiff base derivatives (**S1-S6**) was evaluated by the paper disc diffusion method [29]. The zones of inhibition were measured on Mueller-Hinton agar for bacterial strains and Sabouraud dextrose agar for fungal strains. The test organisms included *S. epidermidis*, *S. aureus*, *E. coli*, *P. aeruginosa*, *A. fumigatus* and *A. niger*. The compounds were prepared in DMF at concentrations of 50 and 100 µg/disc. The impregnated discs were placed on inoculated agar plates and incubated at 37 ºC for 24 h for bacteria and 48 h for fungi. Ciprofloxacin (100 µg/disc) and fluconazole (100 µg/disc) were used as reference drugs for antibacterial and antifungal activity, respectively. DMF served as the solvent control. The antimicrobial activity was determined by comparing the zones of inhibition with those of the respective reference drugs.

Minimum inhibitory concentration (MIC): The MIC of the synthesized compounds was determined using the broth microdilution method according to CLSI guidelines [30]. Serial two-fold dilutions of each compound were prepared in sterile Mueller–Hinton broth for bacteria and appropriate fungal broth for fungi. A standardized microbial suspension (~5×10^5 CFU/mL) was added to each well of a sterile 96-well microtiter plate. Growth, sterility, solvent and standard drug controls were included. Following incubation at 37 ºC for bacteria (18-24 h) and 28-35 ºC for fungi (48 h), the MIC was recorded as the lowest concentration showing complete inhibition of visible microbial growth.

Anti-inflammatory activity: Animals were weighed and randomly assigned to four groups (n = 3/group). They were fasted overnight for 12-16 h with free access to water before the experiment. Baseline paw thickness of the right hind paw was measured at 0 h at a consistent dorsoventral landmark, just proximal to the metatarsophalangeal joint. Test compounds and vehicle were administered orally (p.o.) by gavage at a dose volume of 10 mL/kg body weight. After 1 h, acute inflammation was induced by sub-plantar injection of turpentine oil (0.1 mL) into the right hind paw. Paw thickness was measured at 1, 2, 3 and 4 h after injection at the same anatomical site. The measurements were recorded in millimetres (mm). All

measurements were performed by the same observer. Data were expressed as mean ± SEM and paw edema and percentage inhibition of edema were calculated for each group at each time point [31].

Anti-pyretic effect: Animals were fasted overnight for 12-18 h with free access to water. Basal rectal temperature (T_0) was recorded using a digital thermometer. Pyrexia was induced by subcutaneous injection of turpentine oil (0.5 mL/rat) into the plantar surface of the right hind paw. After 3 h, rectal temperature was recorded again and animals showing an increase of ≥ 0.5 ºC were considered pyretic and included in the study. Test compounds were administered orally by gavage at 3 h, designated as 0 h for treatment. Rectal temperature was recorded at 0, 1, 2, 3 and 4 h after treatment. The results were expressed as mean ± SEM for each group [32].

RESULTS AND DISCUSSION

The thiazole-Schiff base derivatives (**S1-S6**) were synthesized by condensation of thiazol-2-amine with the corresponding aromatic aldehydes in glacial acetic acid. Formation of the azomethine (–CH=N–) linkage was supported by the characteristic FT-IR and ^{1}H NMR signals, while MS and elemental analysis were consistent with the proposed molecular formulas. The substituent pattern, particularly the hydroxyl and methoxy groups in **S5** and **S6**, provides additional hydrogen-bonding sites that may influence their subsequent biological activity.

Molecular docking studies: Molecular docking was performed to examine the interactions of Schiff base derivatives **S1-S6** with *S. aureus* DNA gyrase B and cyclooxygenase-2 (COX-2) (Table-1). The docking scores varied among the synthesized compounds, with more negative values representing stronger predicted ligand–protein interactions. Against DNA gyrase B, compound **S6** showed the highest predicted affinity with a docking score of -9.0 kcal/mol, followed by compound **S1** (-8.9 kcal/mol), compared with -9.5 kcal/mol for ciprofloxacin. The ligands were accommodated within the active-site cavity through hydrogen bonding and hydrophobic interactions with surrounding amino acid residues.

TABLE-1
BINDING AFFINITY OF THIAZOLE-BASED SCHIFF BASE AGAINST *Staphylococcus aureus* DNA GYRASE B AND CYCLOOXYGENASE 2 PROTEIN

Compound	*Staphylococcus aureus* DNA gyrase B Protein	Cyclooxygenase 2 protein
S1	-8.9	-9.2
S2	-6.5	-7.2
S3	-7.0	-6.8
S4	-7.6	-6.1
S5	-8.1	-8.3
S6	-9.0	-9.4
Ciprofloxacin	-9.5	–
Diclofenac sodium	–	-9.8

Compound **S5** showed an intermediate docking score of -8.1 kcal/mol, while compounds **S2**, **S3** and **S4** showed weaker predicted interactions.

A similar trend was also observed for COX-2. Compound **S6** exhibited the most favourable docking score (-9.4 kcal/mol), followed by compound **S1** (-9.2 kcal/mol), compared with -9.8 kcal/mol for diclofenac sodium. Compound **S5** showed a docking score of -8.3 kcal/mol, whereas compounds **S2**, **S3** and **S4** displayed weaker interactions. The electrostatic surface representations showed complementary regions of positive and negative electrostatic potential around the ligands and receptor binding sites, supporting the predicted accommodation of the compounds within the respective cavities. The molecular interactions of all synthesized derivatives with the target proteins are shown in Fig. 1.

The docking order against DNA gyrase B was **S6** > **S1** > **S5** > **S3** > **S4** > **S2**, while the order for COX-2 was **S6** > **S1** > **S5** > **S2** > **S3** > **S4**. The stronger predicted binding of **S6** and **S1** may arise from the combination of heterocyclic and electron donating substituents, which provide favourable sites for hydrogen bonding, hydrophobic contacts and electrostatic interactions within the binding pockets. The docking results indicate compounds **S6** and **S1** as the most promising members of the synthesized series for antimicrobial and anti-inflammatory investigation.

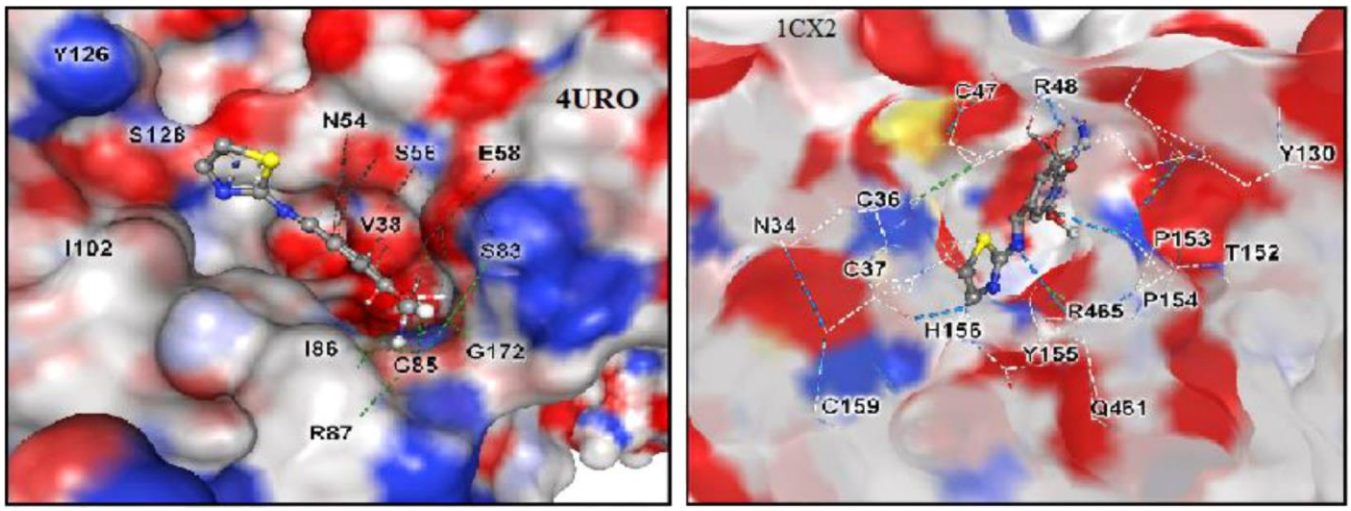

Fig. 1. Docking images of **S6** compound with *Staphylococcus aureus* DNA gyrase B and cyclooxygenase 2 protein

Antimicrobial activity: The antimicrobial activity of compounds **S1-S6** was evaluated against the Gram-positive bacteria *S. epidermidis* and *S. aureus*, Gram-negative bacteria *P. aeruginosa* and *E. coli* and fungal strains *A. fumigatus* and *A. niger* using the zone-of-inhibition assay. The compounds displayed activity of varying magnitude against the tested organisms (Table-2).

Compound **S6** exhibited the highest antibacterial inhibition zones, measuring 28 mm against *S. epidermidis* and *E. coli*, 27 mm against *P. aeruginosa* and 25 mm against *S. aureus*. S1 was the next most active derivative, with inhibition zones of 26, 26, 25 and 24 mm against *S. epidermidis*, *E. coli*, *P. aeruginosa* and *S. aureus*, respectively. Against the fungal strains, compound **S6** gave inhibition zones of 19 mm for *A. fumigatus* and 18 mm for *A. niger*, while compound **S1** gave 17 and 16 mm, respectively. The reference drugs ciprofloxacin and fluconazole showed inhibition zones of 29-32 and 21-22 mm, respectively. Compounds **S3**, **S4** and **S5** exhibited moderate activity, while compound **S2** showed the lowest activity, with inhibition zones of 18-19 mm against the bacterial strains and 10-11 mm against the fungal strains.

The MIC data were consistent with the zone of inhibition results (Table-3). Compound **S6** exhibited the lowest MIC values among the synthesized compounds against the tested bacterial and fungal strains, followed by compounds **S1** and **S5**. Compound **S2** showed the highest MIC values. Ciprofloxacin and fluconazole retained the strongest activity among the reference compounds. The higher activity of compounds **S6** and **S1** may be related to structural features that favour interaction with microbial targets and membrane penetration. The antimicrobial ranking obtained experimentally is in agreement with the docking results against DNA gyrase B, where compounds **S6** and **S1** occupied the first two positions.

Anti-inflammatory activity: The anti-inflammatory activity of synthesized compounds **S1-S6** was evaluated using the turpentine oil-induced paw edema model. Paw edema was measured at 1, 2, 3, 4 and 5 h and compared with the control and indomethacin-treated groups (Tables 4 and 5).

All synthesized compounds reduced paw edema to different extents. Compound **S6** exhibited the strongest activity among the synthesized derivatives, with paw edema values of 0.26 ± 0.013, 0.39 ± 0.015, 0.26 ± 0.024, 0.31 ± 0.035 and 0.34 ± 0.027 cm at 1, 2, 3, 4 and 5 h, respectively. The corresponding values for indomethacin were 0.24 ± 0.016, 0.35 ± 0.027, 0.21 ± 0.043, 0.25 ± 0.015 and 0.30 ± 0.014 cm. Compound **S1** showed the next highest activity, while compound **S5** displayed moderate activity, whereas compounds **S2**, **S3** and **S4** were less active.

Compound **S6** showed percentage inhibition of edema of 12.28%, 14.39%, 15.92%, 20.31% and 22.37% at 1, 2, 3, 4 and 5 h, respectively. The activity of compound **S6** is consistent with its favourable COX-2 docking score (-9.4 kcal/mol). Its methoxy and hydroxyl substituents may contribute to hydrogen-bonding and other non-covalent interactions within the target binding site. The experimental anti-inflammatory activity and docking results both place compounds **S6** and **S1** among the most active derivatives, although enzyme inhibition studies would be required to establish a direct COX-2 inhibitory mechanism.

TABLE-2
ZOI (mm) OF SYNTHESIZED THIAZOLE-BASED SCHIFF BASE COMPOUNDS AGAINST DIFFERENT PATHOGENS

Compounds	*S. epidermidis*	*S. aureus*	*P. aeruginosa*	*E. coli*	*A. fumigatus*	*A. niger*
S1	26	24	25	26	17	16
S2	19	18	18	19	11	10
S3	22	20	19	21	13	12
S4	20	19	18	20	13	12
S5	24	22	22	23	14	13
S6	28	25	27	28	19	18
Ciprofloxacin (100 μg/disc)	31	29	32	32	–	–
Fluconazole (100 μg/disc)	–	–	–	–	21	22
Control	01	–	–	–	01	–

Values represent the mean zone of inhibition (mm) of three independent experiments performed in triplicate (n = 3).

TABLE-3
MIC OF SYNTHESIZED THIAZOLE-BASED SCHIFF BASE COMPOUNDS AGAINST DIFFERENT PATHOGENS

Compounds	*S. epidermidis* (μg/mL)	*S. aureus* (μg/mL)	*P. aeruginosa* (μg/mL)	*E. coli* (μg/mL)	*A. fumigatus* (μg/mL)	*A. niger* (μg/mL)
S1	8	8	8	8	32	32
S2	32	32	32	32	128	128
S3	16	16	32	16	64	64
S4	32	32	32	32	64	64
S5	8	16	16	16	64	64
S6	4	8	4	4	16	16
Ciprofloxacin (100 μg/disc)	2	2	1	1	–	–
Fluconazole (100 μg/disc)	–	–	–	–	8	8
Control	–	–	–	–	–	–

Values represent the mean minimum inhibitory concentration of three independent experiments performed in triplicate (n = 3).

TABLE-4
TURPENTINE OIL-INDUCED PAW OEDEMA VOLUME OF WISTAR RAT AFTER ADMINISTRATION OF THE THIAZOLE BASED SCHIFF BASE DERIVATIVES (**S1-S6**)

Compounds	Paw volume (cm)				
	1 h	2 h	3 h	4 h	5 h
S1	0.29 ± 0.013**	0.42 ± 0.009 **	0.29 ± 0.045**	0.34 ± 0.018**	0.39 ± 0.037**
S2	0.32 ± 0.008**	0.49 ± 0.026**	0.36 ± 0.032**	0.42 ± 0.017**	0.45 ± 0.015**
S3	0.33 ± 0.005**	0.53 ± 0.009**	0.40 ± 0.006**	0.46 ± 0.005**	0.47 ± 0.022**
S4	0.35 ± 0.005*	0.57 ± 0.011*	0.43 ± 0.013*	0.50 ± 0.009*	0.52 ± 0.013*
S5	0.30 ± 0.011**	0.45 ± 0.012**	0.32 ± 0.026**	0.38 ± 0.009**	0.42 ± 0.026**
S6	0.26 ± 0.013*	0.39 ± 0.015*	0.26 ± 0.024*	0.31 ± 0.035*	0.34 ± 0.027*
Control	0.38 ± 0.012	0.71 ± 0.023	0.74 ± 0.052	0.70 ± 0.028	0.69 ± 0.010
Indomethacin (10 mg/kg)	0.24 ± 0.016*	0.35 ± 0.027**	0.21 ± 0.043**	0.25 ± 0.015**	0.30 ± 0.014*

**$p < 0.05$, *$p < 0.01$as compared to blank and standard respectively. Statistical analysis- One way ANOVA.

TABLE-5
PERCENTAGE INHIBITION OF PAW THICKNESS AFTER ADMINISTRATION OF THE THIAZOLE BASED SCHIFF BASE DERIVATIVES (**S1-S6**)

Compounds	Paw thickness (%)				
	1 h	2 h	3 h	4 h	5 h
S1	11.54 ± 0.004**	13.75 ± 0.005*	14.92 ± 0.003*	19.26 ± 0.003**	21.42 ± 0.004*
S2	10.22 ± 0.003**	11.74 ± 0.009**	12.81 ± 0.007*	17.45 ± 0.005*	19.26 ± 0.006**
S3	09.67 ± 0.011**	11.18 ± 0.003*	12.04 ± 0.008**	16.79 ± 0.008**	18.42 ± 0.011*
S4	09.25 ± 0.012*	10.42 ± 0.012*	11.38 ± 0.009*	16.21 ± 0.006*	18.03 ± 0.013**
S5	10.87 ± 0.016*	12.05 ± 0.011*	13.27 ± 0.011*	18.39 ± 0.012**	20.36 ± 0.015**
S6	12.28 ± 0.012**	14.39 ± 0.012**	15.92 ± 0.013*	20.31 ± 0.012*	22.37 ± 0.012*
Control	0	0	0	0	0
Indomethacin (10 mg/kg)	13.68 ± 0.009*	16.54 ± 0.003**	18.39 ± 0.012**	22.71 ± 0.006**	25.48 ± 0.007*

**$p < 0.05$, *$p < 0.01$as compared to blank and standard respectively. Statistical analysis- One way ANOVA.

Antipyretic activity: The antipyretic activity of the synthesized compounds **S1-S6** was assessed by measuring rectal temperature in pyretic rats at 0, 1, 2, 3 and 4 h after treatment (Table-6). Compound **S1** reduced rectal temperature from 38.6 ± 0.15 ºC at 0 h to 37.4 ± 0.12 ºC after 4 h, while compound **S6** reduced the temperature from 38.6 ± 0.11 ºC to 37.8 ± 0.08 ºC. Indomethacin reduced the temperature from 38.6 ± 0.11 ºC to 37.1 ± 0.13 ºC. Compound **S5** showed moderate activity, reaching 38.1 ± 0.09 ºC after 4 h, whereas compounds **S2**, **S3** and **S4** showed comparatively weak effects.

The antipyretic response of compounds **S1** and **S6** is consistent with their anti-inflammatory profiles. Reduction of fever may be associated with modulation of prostaglandin-mediated pathways involved in hypothalamic temperature regulation. A direct mechanism cannot be assigned from the present data alone, but the biological response supports further investigation of these derivatives.

Structure–activity relationship: The biological data indicate that the nature of the substituents on the thiazole-Schiff base framework has an important effect on activity. Compound **S6** exhibited the strongest antimicrobial and anti-inflammatory profiles and the most favourable docking scores against DNA gyrase B and COX-2. The presence of methoxy and hydroxyl substituents may favour hydrogen bonding and hydrophobic interactions while influencing the electronic and lipophilic properties of the molecule. Compound **S1** having a furan moiety showed the second strongest antimicrobial profile

TABLE-6
RECTAL TEMPERATURE (ºC) OF WISTAR RAT AFTER ADMINISTRATION OF THE THIAZOLE BASED SCHIFF BASE DERIVATIVES (**S1-S6**)

Compounds	Rectal temperature (ºC)				
	0 h	1 h	2 h	3 h	4 h
S1	38.6 ± 0.11	38.2 ± 0.15**	38.0 ± 0.16**	37.8 ± 0.09**	37.8 ± 0.08**
S2	38.6 ± 0.06	38.5 ± 0.13**	38.4 ± 0.09**	38.3 ± 0.08**	38.4 ± 0.06**
S3	38.6 ± 0.17	38.6 ± 0.14	38.6 ± 0.13	38.5 ± 0.13	38.7 ± 0.11
S4	38.6 ± 0.13	38.7 ± 0.14	38.7 ± 0.11	38.8 ± 0.15	38.9 ± 0.15
S5	38.6 ± 0.09	38.3 ± 0.13**	38.1 ± 0.07**	38.1 ± 0.05**	38.1 ± 0.09**
S6	38.6 ± 0.15	38.1 ± 0.09*	37.9 ± 0.08*	37.5 ± 0.10**	37.4 ± 0.12**
Control	38.6 ± 0.12	38.9 ± 0.14	39.2 ± 0.15	39.4 ± 0.13	39.5 ± 0.14
Indomethacin	38.6 ± 0.11	37.9 ± 0.12**	37.6 ± 0.14*	37.3 ± 0.12**	37.1 ± 0.13**

**$p < 0.05$, *$p < 0.01$as compared to blank and standard respectively. Statistical analysis- One way ANOVA.

and favourable activity in the anti-inflammatory and anti-pyretic models. Its docking scores against DNA gyrase B (-8.9 kcal/mol) and COX-2 (-9.2 kcal/mol) were close to those of compound **S6**.

Compound **S5** displayed intermediate biological and docking activity, whereas compounds **S2**, **S3** and **S4** generally showed weaker responses. The comparable trends observed in antimicrobial screening, MIC values, anti-inflammatory activity and molecular docking support a relationship between substitution pattern and biological response. The present SAR findings identify compounds **S6** and **S1** as the most promising derivatives of the series and provide a basis for further structural modification and biological evaluation.

Conclusion

The present study describes the synthesis and biological evaluation of thiazole-based Schiff base derivatives (**S1-S6**) for antimicrobial, anti-inflammatory and antipyretic activities. Among the synthesized compounds, **S6** and **S1** exhibited the strongest biological activity and favourable docking scores against *S. aureus* DNA gyrase B and COX-2. Both compounds showed good antibacterial and antifungal activity, while compounds **S6** and **S1** reduced paw edema and elevated body temperature in the respective animal models. Their enhanced activity may be related to the heterocyclic framework and the presence of methoxy and hydroxyl substituents, which can influence hydrogen bonding and lipophilic interactions.

CONFLICT OF INTEREST

The authors declare that there is no conflict of interests regarding the publication of this article.

DECLARATION OF AI-ASSISTED TECHNOLOGIES

During the preparation of this manuscript, the authors used an AI-assisted tool(s) to improve the language and no data, results or scientific conclusions were generated by AI. All analyses, interpretations and conclusions are the authors' own. The authors reviewed and edited the content and take full responsibility for the published work.

REFERENCES

1. Z.X. Niu, Y.T. Wang, S.N. Zhang, Y. Li, X.B. Chen, S.Q. Wang and H.M. Liu, *Eur. J. Med. Chem.*, **250**, 115172 (2023); https://doi.org/10.1016/j.ejmech.2023.115172
2. M.F. Arshad, A. Alam, A.A. Alshammari, M.B. Alhazza, I.M. Alzimam, M.A. Alam, G. Mustafa, M.S. Ansari, A.M. Alotaibi, A.A. Alotaibi, S. Kumar, S.M.B. Asdaq, M. Imran, P.K. Deb, K.N. Venugopala and S. Jomah, *Molecules*, **27**, 3994 (2022); https://doi.org/10.3390/molecules27133994
3. M.T. Chhabria, S. Patel, P. Modi and P.S. Brahmkshatriya, *Curr. Top. Med. Chem.*, **16**, 2841 (2016); https://doi.org/10.2174/1568026616666160506130731
4. A. Khamitova, D. Berillo, A. Lozynskyi, Y. Konechnyi, D. Mural, V. Georgiyants and R. Lesyk, *Mini Rev. Med. Chem.*, **24**, 531 (2024); https://doi.org/10.2174/1389557523666230713115947
5. D.H. Dawood, S.A. Al-Hussain, T.A. Farghaly, A.M.R. Alsaedi and M.E.A. Zaki, *RSC Adv.*, **16**, 31009 (2026); https://doi.org/10.1039/D6RA02615J
6. I.P. Singh, S. Gupta and S. Kumar, *Med. Chem.*, **16**, 4 (2020); https://doi.org/10.2174/1573406415666190614101253
7. X. Zhao, J. Di, D. Luo, R. Verma, S.K. Verma, S. Verma, L. Ravindar, A. Koshle, H.K. Dewangan, R. Gupta, S. Chandra, S. Deshpande, Kamal, Y. Vaishnav and K.P. Rakesh, *Bioorg. Chem.*, **154**, 108035 (2025); https://doi.org/10.1016/j.bioorg.2024.108035
8. T.A. Farghaly, A.M.R. Alsaedi, N.A. Alenazi and M.F. Harras, *Expert Opin. Ther. Pat.*, **32**, 791 (2022); https://doi.org/10.1080/13543776.2022.2067477
9. H. Saini, A. Mehra and A. Mittal, *Future Med. Chem.*, **17**, 2021 (2025); https://doi.org/10.1080/17568919.2025.2550929
10. S. Nagar, S. Raizada and N. Tripathee, *Result Chem.*, **6**, 101153 (2023); https://doi.org/10.1016/j.rechem.2023.101153
11. S. Kumar, G. Jashi, Shakti, Y. Khajuria and A. Agarwal, *J. Mol. Struct.*, **1358**, 145279 (2026); https://doi.org/10.1016/j.molstruc.2026.145279
12. E. Raczuk, B. Dmochowska, J. Samaszko-Fiertek and J. Madaj. *Molecules*, **27**, 787 (2022); https://doi.org/10.3390/molecules27030787
13. I. Mushtaq, M. Ahmad, M. Saleem and A. Ahmed, *Future J. Pharm. Sci.*, **10**, 16 (2024); https://doi.org/10.1186/s43094-024-00594-5
14. G. Venkatesh, P. Vennila, S. Kaya, S.B. Ahmed, P. Sumathi, V. Siva, P. Rajendran and C. Kamal, *ACS Omega*, **9**, 8123 (2024); https://doi.org/10.1021/acsomega.3c08526
15. S. Yadav, A. Kamboj, A. Yadav and K. Poonia, *RSC Adv.*, **16**, 41205 (2026); https://doi.org/10.1039/D6RA03746A
16. E Alterhoni, A. Tavman, D. Gurbuz, M. Hacioglu, A. Cinarli, O. Sahin and A.S.B. Tan, *ChemistrySelect*, **5**, 9730 (2020); https://doi.org/10.1002/slct.202001498
17. X. Zhang, H. Fan, Q. Chen, L. Pan and L. Jin, *J. Agric. Food Chem.*, **73**, 22162 (2025); https://doi.org/10.1021/acs.jafc.5c01912
18. S. Kaushik, S.K. Paliwal, M.R. Iyer and V.M. Patil, *Med. Chem. Res.*, **32**, 1063 (2023); https://doi.org/10.1007/s00044-023-03068-0
19. G. Matela, *Anti-Cancer Agents Med. Chem.*, **20**, 1908 (2020); https://doi.org/10.2174/1871520620666200507091207
20. S.J. Hamid and T. Salih. *Drug Des. Dev. Ther.*, **16**, 2275 (2022); https://doi.org/10.2147/DDDT.S364746
21. M.S. Rana, N.M.A. Rayhan, M.S.H. Emon, M.T. Islam, K. Rathry, M.M. Hasan, M.M. Islam Mansur, B.C. Srijon, M.S. Islam, A. Ray, M.A. Rakib, A. Islam, M. Kudrat-E-Zahan, M.F. Hossen and M.A. Asraf, *RSC Adv.*, **14**, 33094 (2024); https://doi.org/10.1039/D4RA04375H
22. M. Rani, J. Devi, B. Kumar and M. Rathi, *Chem. Asian J.*, **19**, e202400676 (2024); https://doi.org/10.1002/asia.202400676
23. A. Mermer, B. Tuzun, S.D. Daştan, U.M. Koçyiğit, F.N. Cetin and O. Cevik, *J. Biochem. Mol. Toxicol.*, **37**, e23465 (2023); https://doi.org/10.1002/jbt.23465
24. K.M. Fahelelbom, A. Saleh, M.M.A. Al-Tabakha and A.A. Ashames, *Rev. Anal. Chem.*, **41**, 21 (2022); https://doi.org/10.1515/revac-2022-0030
25. J. Eberhardt, D. Santos-Martins, A.F. Tillack and S. Forli, *J. Chem. Inf. Model.*, **61**, 3891 (2021); https://doi.org/10.1021/acs.jcim.1c00203
26. J.I. Al-Hawarin, A.A. Abu-Yamin, A.A.A. Abu-Saleh, I.A.M. Saraireh, M.H. Almatarneh, M. Hasan, O.M. Atrooz and Y. Al-Douri, *Materials*, **16**, 5160 (2023); https://doi.org/10.3390/ma16145160
27. C.Y. Hsu, A.R. AlBajalan, S.A. Awad, M. Suliman, C. Rodriguez-Benites, N. Juraev, H. Al-Mohamadi and A.J. Kadhim, *Nanoscale Adv.*, **6**, 6408 (2024); https://doi.org/10.1039/D4NA00642A
28. P. Krishnamoorthy and N. Karthika, *J. Lab. Anim. Sci.*, **6**, 25 (2023); https://doi.org/10.48165/jlas.2023.6.2.4
29. A.M. Asiri and S.A. Khan, *Molecules*, **15**, 6850 (2010); https://doi.org/10.3390/molecules15106850
30. N.C. Rocha, J.M. Lopes, K.L. Russi, J.K. Palmeiro and R. Girardello. *Front. Cell. Infect. Microbiol.*, **13**, 1139784 (2023); https://doi.org/10.3389/fcimb.2023.1139784
31. V.G. Prasad, Ch. Vivek, P. Anand Kumar, P. Ravi Kumar and G.S. Rao, *Eur. J. Drug Metab. Pharmacokinet.*, **40**, 23 (2015); https://doi.org/10.1007/s13318-013-0172-7
32. N.K. Saini and M. Singhal, *Asian Pac. J. Trop. Biomed.*, **2**, 870 (2012); https://doi.org/10.1016/S2221-1691(12)60245-7